buildings

MDPI

Article

Continuous Monitoring of Elastic Modulus of Mortars Using a Single-Board Computer and Cost-Effective Components

Thomas Russo [1,*], Renan Rocha Ribeiro [1], Amir Araghi [2], Rodrigo de Melo Lameiras [2], José Granja [1] and Miguel Azenha [1]

[1] Department of Civil Engineering, University of Minho, ISISE, ARISE, 4800-058 Guimarães, Portugal
[2] Departamento de Engenharia Civil e Ambiental, Universidade de Brasília, Brasília 70910-900, Brazil
* Correspondence: thomas.russo@civil.uminho.pt

Abstract: The Elastic Modulus Measurement through Ambient Response Method (EMM-ARM) is designed to continuously monitor the elastic modulus of hardening construction materials such as concrete, cement paste, mortars, stabilized soils, and epoxy resin. In practice, a composite beam, made of the tested material in its mould, is induced to vibration by means of environmental or controlled excitation, and its resonant frequency is identified. The material's elastic modulus can then be calculated based on the vibration equation of structural systems. The traditional system to conduct EMM-ARM experiments is based on specialized equipment and on proprietary licensed software, which results in a considerable cost, as well as limited options for customization. The paper hereby presented proposes a delve into the development and validation of a cost-effective and open-source system that is able to conduct EMM-ARM experiments. By using a Raspberry Pi for the computing device and cost-effective electronic components, the cost of the system was one-twentieth of the traditional one, without compromising the measurement reliability. The composite beam's excitation is generated, while the vibration response is recorded by the proposed system simultaneously, since the Raspberry Pi supports multiprocessing programming techniques. The flexibility earned by the exclusive use of open-source and cost-effective resources creates countless application possibilities for the proposed system.

Keywords: open-source; cost-effective; elastic modulus; monitoring; hardening construction materials

Citation: Russo, T.; Ribeiro, R.R.; Araghi, A.; Lameiras, R.d.M.; Granja, J.; Azenha, M. Continuous Monitoring of Elastic Modulus of Mortars Using a Single-Board Computer and Cost-Effective Components. *Buildings* **2023**, *13*, 1117. https://doi.org/10.3390/buildings13051117

Academic Editors: Amir Si Larbi and Chiara Bedon

Received: 2 March 2023
Revised: 23 March 2023
Accepted: 13 April 2023
Published: 22 April 2023

1. Introduction

The Elastic modulus (E-modulus) is a key parameter in the mechanical behaviour of materials and structures, and it is especially relevant in the field of civil engineering.

The measurement of E-modulus is particularly important for the hardening of materials used in critical applications, such as high-rise concrete buildings or special engineering structures. In these cases, Ultra- High Performance Concrete (UHPC) and Ultra High Performance Mortar (UHPM) are commonly employed. The ability to accurately measure the E-modulus development since early ages of these materials is essential in predicting their mechanical behaviour over time and ensuring their structural integrity [1–5].

The Elastic Modulus Measurement through the Ambient Response Method (EMM-ARM) was designed to continuously monitor the E-modulus of concrete from the early ages [6]. Originally, the test consisted of a composite beam in simply supported conditions made up of a mould filled with the material being tested and continuously analysed through modal identification methods. The composite beam was excited by environmental noise (e.g., noises from a construction site, voices, wind, etc.), which can be conceptualized as white noise or a random process with constant spectral intensity across all frequencies [7]. Vibrations were measured in the vertical direction using an accelerometer attached to the midpoint of the beam. After the determination of the system's resonant frequency, it was possible to infer the tested material's stiffness (material filled inside the mould) by referring

to the vibration equation of the simply supported structural systems, considering that the mass, geometry, and stiffness of the mould were known [8]. The method allowed for the direct and quantitative estimation of the tested material's E-modulus without any dependence on the data processing by the user [9]. The composite beam was highly excitable due to its slenderness, and could be induced to vibrate by the environmental noise alone. However, the airflow from a fan placed nearby was used to increase the vibration amplitude, improve the signal-to-noise ratio, and facilitate the resonant frequency [10,11]. In this paper, this original version of the EMM-ARM will be referred to as the "traditional EMM-ARM system".

In order to ensure the measurement quality of the EMM-ARM, the method was developed around specialized equipment with high sensitivity which included accelerometers and a data acquisition system. A computer was also necessary, with the proprietary licensed software LabView used to interact with the data acquisition system. Hence, the traditional *EMM-ARM* system has a considerable cost, requiring specialised equipment and licenses to operate. This can be a barrier to access for many researchers and practitioners, particularly those in resource-limited situations.

Research towards the development of a low-cost EMM-ARM device was conducted in [12], where a low-cost EMM-ARM system was developed around a microcontroller, and was able to conduct cement paste tests. In this work, a 16-bit ADC [13] with a maximum sampling rate of 860 Hz as well as an accelerometer with a resolution of 1.2 mg at 60 Hz was used [14]. The limits of this device were found in terms of computing power, as the memory capacity of the microcontroller was reached, and the post-processing routine must be conducted after the experiment on an external computer. This work has, however, started to pave the way for reducing the costs of applying the EMM-ARM method and promoting its dissemination, while highlighting some limits of low-cost electronic components. In this paper, this low-cost version of the EMM-ARM will be referred to as the "MC EMM-ARM system", as it was developed with a microcontroller board.

The hereby presented work has the objective of: (i) reporting the development of an open-source EMM-ARM system that utilizes cost-effective electronics, and (ii) experimentally validating the viability of the proposed system for cement paste and mortar applications by comparing the obtained results with those obtained with a traditional system. Hence, a delve into the proposed system's design is presented, including the choice of components and data processing aspects. The results of the validation tests are presented and discussed in the latter sections. It is, however, stated that this is proof-of-concept work in which extensive metrological validation was not sought. The focus was instead directed to the explanation of the system and the demonstration of a performance similar to the one of the traditional system.

The proposed system follows the same vision as the previously referenced research, with the mean of leveraging the identified limits. The adoption of open-source development methods brings many advantages, such as increased collaboration among developers and researchers; the rapid development and encouragement of creativity and innovative solutions [15]; the elimination of costly proprietary software licenses; greater customization and scalability to tailor the system to their specific needs [16], which is reinforced by the use of cost-effective electronic components; and, lastly, the promotion of transparency and accountability, as the source code and other resources are openly available for review and inspection, thus fostering trust and confidence in the development process. In this vision, the totality of the design documentation together with the codes used in this work will be publicly shared on the platform GitHub through the link available in [17], after the publication of this article.

The cost-effective development boards can be divided into two categories of boards: microcontrollers and Single-Board Computers (SBCs). Overall, SBCs are suitable for multipurpose applications that require heavy processing power, such as multiprocessing tasks, while microcontrollers are focused on specific tasks such as controlling motors, reading sensors, or communicating with other devices. Considering the targeted application,

SBCs were considered more adequate to be used as the computing device. Indeed, as the computing device oversees the monitoring aspects, including data storage and post-processing, the processing power required is relatively high. Furthermore, the authors aim for modularity and adaptability, so any independent user can customize the system to their specific needs. Therefore, the system should be capable of functionalities such as displaying data in graphs and tables during tests or publishing data to an online database in real time. SBCs are suitable for these use cases, as they usually come with relatively high processing power, a large memory capacity, video interfaces such as HDMI, and embedded Wi-Fi/Bluetooth connectivity.

The market for SBCs in research is largely represented by the SBC Raspberry Pi (RPi). As a matter of fact, when comparing the yearly number of publications in Scopus, BeagleBone and Odroid, two of the most serious competitors to the RPi, obtained a maximum of 47 and 46 publications per year between 2012 and 2022, respectively, while the RPi topped out at over 1800 publications in a single year (2019). The RPi is used in a variety of areas, as shown in Table 1, which highlights the high flexibility and modularity offered by the RPi *.

Table 1. The repartition of the RPi's applications, with data from Scopus.

Area	Computer Science	Engineering	Mathematics	Physics & Astronomy	Decision Science	Others
Related publications (Scopus)	31.4%	25%	8%	7.9%	5.4%	22.3%

* Percentages determined by performing a Scopus search in January 2023 for all publications containing the terms "Raspberry Pi" or "RaspberryPi" or "RPi" in their title, abstract or keywords in all years up to 2022, filtering by scientific field.

The consequence of this domination is the availability of a wide community support among RPi users, as well as a large choice of compatible modules specially designed to meet the RPi specifications (RPi Hats). For these advantageous reasons, the choice of the computing device for the EMM-ARM system was a Raspberry Pi 4 model B.

The novelties of the proposed work compared to the MC EMM-ARM system are (i) an SBC is used for the computational tasks, (ii) electronic components with higher specifications which allow improved sensitivity and flexibility while maintaining cost effectiveness, (iii) the system supports controlled excitation generation, both for mortar and concrete applications, (iv) the measurements and post-processing are handled by the system in real-time, and (v) the higher scalability and flexibility for different adaptations.

In comparison with the traditional EMM-ARM system, the innovations of this research are (i) the exclusive use of open-source resources, (ii) the tremendous cost reductions, and (iii) the higher scalability and flexibility for different adaptations.

To validate the reliability and robustness of the proposed EMM-ARM system, experiments on cement paste and mortar were conducted, and the results were compared to those obtained with a traditional EMM-ARM system. The results demonstrated that the proposed EMM-ARM system is a reliable and cost-effective alternative to the traditional one for measuring the elastic modulus of cement pastes and mortars. The system was not tested on concrete specimens; however, as the usual concrete specimen moulds have a ratio EI/L (with E corresponding to the E-modulus, I corresponding to the moment of inertia, and L corresponding to the span) in the same order as mortar specimens, it is expected that the developed system presents a similar performance [18]. The encouraging results obtained with the proposed system and the flexibility that it offers allow many future application possibilities, such as the continuous characterization of cement, lime, or cement-lime composite materials or air-lime mortars, the quality control of hardening construction materials, and the application to other hardening materials, such as epoxy resins. The derived applications of the system could also include rheological measurements of fresh materials. This paper is structured around five sections, including the present introduction, in a way that the reader is firstly acquainted with the intricacies of the traditional system

(Section 2. The proposed EMM-ARM system is then detailed (Section 3), followed by its experimental validation (Section 4). The final remarks are delivered in Section 5.

2. Review of the Traditional EMM-ARM System

Since the creation of the EMM-ARM, the method was subjected to extensive research, and was successfully adapted to monitor the E-modulus evolution of mortars [19], stabilized soils [20], cement paste [21], and epoxy resins [22]. Through those past research works, considerable improvements were brought both to the setup and to the procedure for data processing, making EMM-ARM a reliable and robust method [18].

The following subsections present the current state of the art regarding (i) the mould geometry for cement paste and mortar specimens; (ii) the excitation source of the specimens under testing; (iii) the electronic setup constituting the EMM-ARM system, and (iv) the modal parameters identification method used.

2.1. Mould Geometry

For the E-modulus characterization of cement paste, the specimens are in cantilever conditions. This cantilever configuration allows the specimen to be easily excitable by the ambient vibration, making this test adequate for Operational Modal Analysis (OMA) [23]. The mould is made of an acrylic tube with internal and external diameters of 16 mm and 20 mm, respectively. The total length of the mould is 550 mm, and the span is 450 mm. The clamping system was specifically designed to meet adequate boundary conditions with these moulds [18]. Figure 1 represents a scheme of the experimental setup for the E-modulus monitoring of cement paste with EMM-ARM.

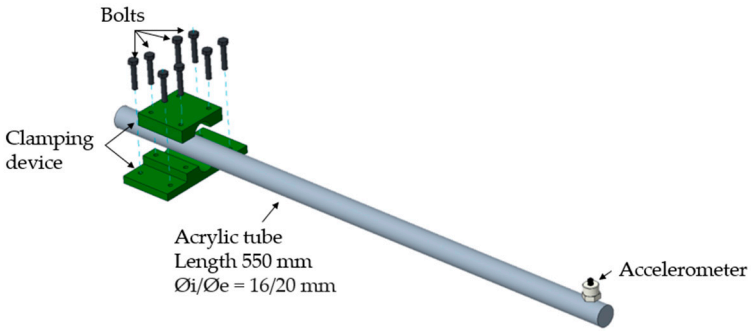

Figure 1. Mould setup for cement paste testing, adapted from [18].

The mortar specimens' setup, on the other hand, is directly inspired by the concrete testing, but was significantly reduced in size, as the characteristic aggregate size in mortar is considerably smaller. Therefore, the mould is in simply supported conditions, and is constituted of a 550 mm long PVC tube with a 44 mm and 50 mm of internal and external diameter, respectively. The span of this beam is 500 mm. The supports for the mortar specimens were directly derived from the supports for concrete specimens, which were thoroughly designed in [18]. Figure 2 represents a scheme of the test setup for mortar testing with the EMM-ARM. The presence of the actuator is explained in the following subsection.

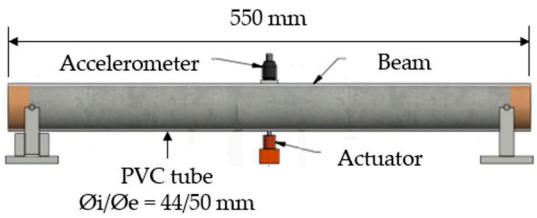

Figure 2. Mould setup for mortar testing, adapted from [18].

2.2. Excitation Source

Initially, as previously mentioned, the specimens under the EMM-ARM test were subjected to environmental vibrations, or to the airflow of a fan, which would create the excitation necessary to induce a measurable vibrating state, corresponding to the Operational Modal Analysis (OMA) testing.

In concrete applications, the initial mould was composed of a 2 m long acrylic tube, with an internal and external diameter of 92 mm and 100 mm, respectively; such dimensions made the casting and manipulation procedures difficult. Therefore, a significant geometrical downsizing was conducted on the moulds. The mould was reduced to a 1-m-long PVC tube, with internal and external diameters of 86 mm and 90 mm, respectively. This geometrical downsizing implied a reduction in the elastic slenderness ratio, making the beam less excitable by the environmental noise and resulting in a lower signal-to-noise ratio in the acceleration measurements, which could eventually compromise the reliability and robustness of the method. Moreover, it was observed that environmental noise, especially in construction sites, can be contaminated by heavy machinery generating significant vibrations at certain frequencies, or a set of frequencies, such as vibrations conducted through the ground or air [24]. To address these issues and conserve the robustness of the EMM-ARM, the experimental technique was converted from OMA to Experimental Modal Analysis (EMA). The conversion was achieved by the generation of a controlled low-intensity excitation through a contactless electromagnetic actuator [24], as shown in Figure 2. The controlled excitation is under the shape of a sine sweep along a set of frequencies corresponding to the resonance frequencies met by the beam as the material was hardening. The amplitude of the sinusoidal signal is constant over all the frequencies so that its power spectrum density over the entire acquisition time is constant on the targeted set of frequencies, as would be the case with white noise [25].

Experiments with EMM-ARM on mortars were chronologically initiated after the completion of these improvements for concrete; mortar applications consequently benefited from this research, and are now commonly conducted with the controlled excitation system [16].

For cement paste testing, however, the methodology of OMA is still used, as the dimensions and mass of the specimens are adequate for ambient vibration excitation, and consistently reliable results are obtained [18].

2.3. Hardware

The electronic hardware used for the traditional EMM-ARM system is still the same as that used for the thorough improvements and validation of the method in [18]. The accelerometers used are from the brand PCB Piezotronics, and several models have been used for EMM-ARM applications, the most common one being the lightweight accelerometer (5.8 g) PCB 352C34 [26]. This accelerometer has a sensitivity of 100 mV/g at a range of $\pm$50 g and a broadband resolution of 0.15 mg rms. The data acquisition system, in charge of converting the analogue readings of the accelerometers to discrete values and also responsible for generating the excitation signal when required, is the NI USB-4431 [27] from the brand National Instruments. This board has a maximum sampling frequency of 102.4 kHz on four channels, and a resolution of 24-bits. The data acquisition system is connected to a computer, which is equipped with LabView software in order to interact with it.

The electromagnetic actuator is a custom-made part, made of a coil and a magnet, as presented in [24]. This coil is made with 3140 turns of a Ø 0.22 mm copper wire, which then forms a coil with internal and external diameters of 10 mm and 25 mm, respectively. The controlled excitation is applied to the coil as an electrical signal, while the cylindrical magnet (a Neodymium N50 magnet with remanence: Br = 1.4 T; Ø = 8 mm; height = 20 mm) is physically attached to the bottom of the mould, at midspan. The other side of the magnet is at the centre of the coil, without any physical contact between the two parties.

The total cost of the traditional EMM-ARM system for applications to two specimens (therefore with two accelerometers) was calculated in December 2022 to value EUR 5000, not including the price of the laptop used.

2.4. Modal Identification

The procedure for the modal identification was also subjected to major improvements through the research on the EMM-ARM. In the initial procedure for the application to concrete, the accelerations were monitored at mid-span in packages of 900 s. The data was then converted from the time domain to the frequency domain through the Welch procedure [28], resulting in the normalized power spectrum density for each package. The resonance frequencies of the first vibration mode were then identified by the highest peak in each amplitude spectrum. To obtain a continuous evolution of the composite beam's resonance frequency, this procedure was repeated every 60 min. Further details related to the initial procedure can be found in [29].

Currently, due to the improvements in the excitation method for concrete and mortars (controlled excitation), the monitoring time for each package of data has been lowered for values between 300 s and 600 s [30]. Cement paste applications also adopted these data acquisition durations, as the excitation levels of the specimens are adequate. The post-processing sequence was also improved for more reliable and robust modal parameter identification, since the Stochastic Subspace Identification (SSI) method is currently used. The SSI method is a time-domain method (also known as the parametric method), therefore it is less sensitive to noise levels and thus more robust than the previous identification method used [31]. This method allows for the identification of the natural frequencies, damping ratios and mode shapes of a system from the measured data. Extensive details regarding the SSI method can be found in [32–34]. The SSI method, in the case of the EMM-ARM, is implemented for OMA tests (cement paste) as an output-only driven method, as well as its variant for EMA tests (concrete and mortars) as an input-output driven method [18].

3. Proposed EMM-ARM System Design

The proposed EMM-ARM system is composed of several electronic components which can be divided into two distinct categories: (i) a data acquisition system, presented in Section 3.1, and (ii) a controlled excitation system, presented in Section 3.2. The different connections and interactions between each component are detailed in Section 3.3. Finally, Section 3.4 presents the intricacies of the software aspects in order to manage the components and conduct EMM-ARM tests.

3.1. Data Acquisition System

The computing device for the development of the proposed EMM-ARM system is the central node; it manages the monitoring functions during the test, as well as the post-processing procedure right after the monitoring phase.

As mentioned in the introduction to this work, in Section 1, the computing device selected for this application is the Raspberry Pi (RPi) 4 model B. This SBC is powered by a Quad-core Cortex-A72 64-bit CPU, running at a maximum frequency rated at 1.5 GHz. The one used for the development of the proposed system integrates 8 GB of SDRAM memory. The board also has four USB ports, two micro-HDMI ports, and 40 Global Purpose Input/Output (GPIO) pins. More details related to the specifications of the RPi can be found in its datasheet [35].

When conducting an EMM-ARM test, the response of the specimen to the excitation (environmental or controlled), corresponding to its vibration, is the key data required to calculate the material's E-modulus. Therefore, the data acquisition hardware of the proposed EMM-ARM system is composed of accelerometers and an analogue to digital Converter (ADC), since RPi does not integrate any built-in ADC [35].

The accelerometer selected for this application is the ADXL203EB from Analog Devices, with a sensitivity of 1000 mV/g, a resolution of 1 mg at 60 Hz, and a measurement range of ±5 g. As a comparison, the accelerometer used in the traditional EMM-ARM system is able to identify changes in acceleration almost seven times smaller than the accelerometer used in this research (the comparison is based on the accelerometers' resolutions). This comparison highlights the tremendous gap of measurement capacities between lower-cost electronic components and specialized equipment. However, this accelerometer is 36% better in terms of resolution than the one used in the MC EMM-ARM system.

In terms of ADC performance requirements, its resolution should be better than the resolution of the accelerometer, so as not to be a limiting element. In practice, the determination of the ADC's resolution is equivalent to determining the minimum resolution in order to measure acceleration changes of 1 mg (accelerometer's resolution). Given that the accelerometer is an analogue sensor, it converts accelerations into a voltage; the relationship between accelerations (input) and voltage (output) is determined by the sensor's sensitivity, which is 1000 mV/g in this case. Therefore, an acceleration change of 1 mg corresponds to an output voltage change of 1 mV. Consequently, the ADC should have a resolution sufficient to read voltage changes smaller than or equal to 1 mV (corresponding to the target ADC voltage resolution). The voltage resolution of an ADC is calculated as:

$$\text{ADC voltage resolution} = \frac{V_H - V_L}{2^n} \quad (1)$$

With V_H and V_L respectively defined as the higher and the lower voltages read by the ADC, and n corresponding to the ADC resolution in bits. Trivially, n can be calculated as

$$n = \log_2\left(\frac{V_H - V_L}{ADC\ voltage\ resolution}\right) \quad (2)$$

The ADC measuring voltages in the range [0; 5] V, n must be superior or equal to 14-bits in order to fully take advantage of the accelerometer's resolution.

Regarding the ADC sampling frequency requirements, the Nyquist-Shannon sampling theorem [36] states that the measurement sampling frequency must be at least twice as big as the highest frequency of the measured signal. In practice, for conservative motives, as well as to ensure a high level of accuracy, to prevent aliasing and to increase the signal-to-noise ratio [37], a factor 4 was used for the design of the system. For the EMM-ARM application, 250 Hz is a safe value to consider as the highest frequency that can be expected during measurements, considering the use of normal materials and specimen types [18]. Therefore, the ADC should allow a sampling frequency of at least 1000 Hz for each channel measured. As the application of the mortar test requires the measurement of the accelerations of the specimen together with the controlled excitation generated, the ADC must be able to acquire two channels at a minimum of 1000 Hz.

On the market of cost-effective ADC boards, only a limited number of models offer an interesting combination of high sampling frequency (over 2000 Hz) and high resolution (over 14-bit). The ADC used in this work is a commercially available ADC board adapted for rapid prototyping, the Waveshare High-Precision AD/DA board [38], which has 8 channels with 24-bit resolution with a maximum sampling frequency rated at 30,000 Hz. This ADC communicates with the RPi through the Serial Peripheral Interface (SPI) protocol [39]. It was, however, observed by the authors that, in practice, the maximum sampling frequency reached by this ADC connected to an RPi is approximately 5000 Hz when only one channel is acquired, and approximately 3500 Hz in total sampling frequency when two channels are simultaneously acquired (1750 Hz on each channel). The ADC therefore allows for the monitoring of a single mortar specimen at a time; when several specimens are to be monitored in the same experiment, their vibrations are measured in sequence. In the ADC proposing eight input channels, up to eight specimens can be monitored in the same test without the addition of supplementary components such as multiplexers.

3.2. Controlled Excitation System

In order to conduct experiments on mortar or concrete specimens, it is necessary to excite them and measure their response to the excitation. To achieve this, a predefined signal must be generated and applied to the actuator, which will be used to excite the specimen. The signal used in this case is a sine sweep, which spans the frequency range of interest (the frequencies expected to be met by the specimen during the experiment; considering the usual materials and specimen types, [20; 250] Hz is a safe range [18]), and is repeated indefinitely during the measurement period.

To generate the analogue signal required for this experiment, a digital-to-analogue Converter (DAC) is employed. In this instance, a 12-bit DAC was selected, the MCP4725 from Adafruit, which uses the Inter-Integrated Circuit (I^2C) communication protocol [39]. This DAC, when connected to an RPi, is capable of generating a sine signal with a frequency of over 800 Hz, which is more than sufficient for this application, as an excitation of up to 250 Hz is required.

A common issue encountered with low-cost DACs is their inability to generate negative voltage signals. In this work, it was important to generate a sine signal that is centered around 0 V in order to obtain a null average force of excitation. The selected DAC suffers from this limitation: the signal at its output pin ranges from 0 V to 5 V. Consequently, the output signal must be shifted down to be centered around 0 V. Another common limitation of low-cost DACs is their weak capacity for current output. As a matter of fact, it was observed that the output signal experiences a voltage drop resulting from a current drop when the DAC is connected to the electromagnetic actuator. The voltage amplitude of a sine sweep signal generated by the DAC when nothing is connected to its output pin is visible in Figure 3a (measured with the ADC). In this figure, it is possible to see that the sine sweep has a voltage amplitude oscillating in the range [0.5; 4.4] V. The actuator was then connected to the output pin of the DAC, and the signal now oscillates in the range of [2.0; 3.9] V in the lower frequencies (0–10 Hz), as can be seen in Figure 3b. When the sine signal's frequency increases, the voltage amplitude increases slightly as well, reaching a maximum range of [1.7; 4.2] V.

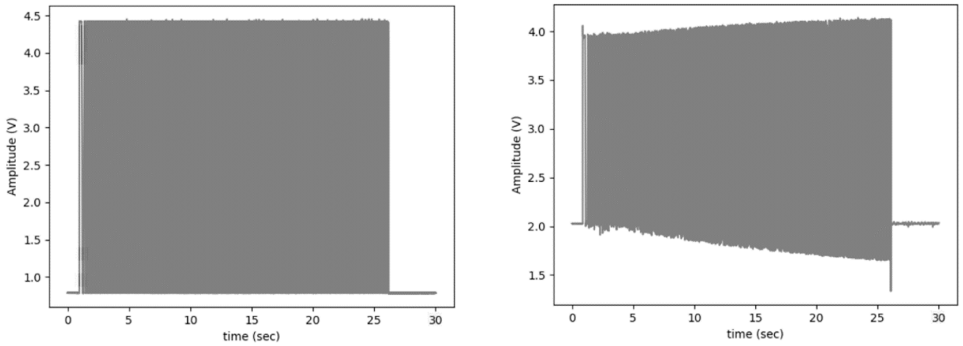

(**a**) (**b**)

Figure 3. Signal voltage from the DAC when (**a**) the actuator was not connected; and (**b**) the actuator was connected.

To address these issues, an amplifying and shifting circuit was designed, which is presented in Figure 4. The circuit is based on two key components: a transistor and an operational amplifier (op-amp). The transistor allows the circuit to supply the actuator from an external power source, which solves the issue of voltage drops. The selected transistor for this application is a TIP 120, which is a Darlington transistor, and is therefore ideal for the present use case [40]. The transistor is in common collector configuration in order to have a voltage gain close to 1, but a considerable current gain.

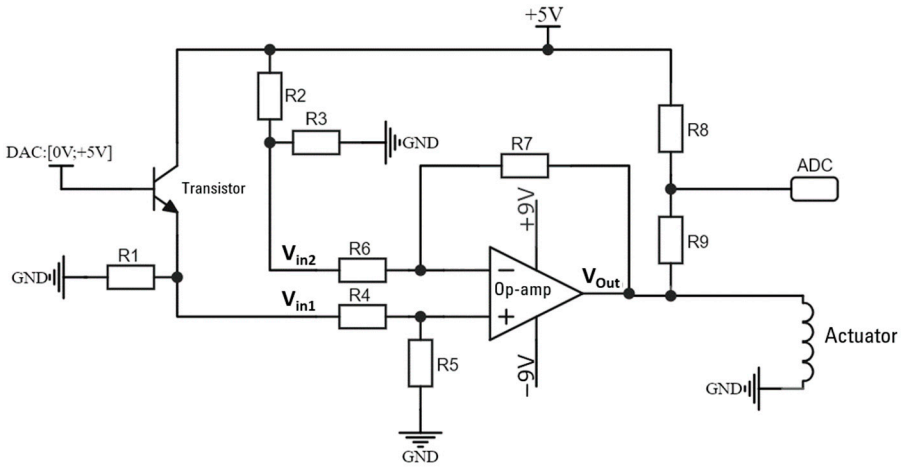

Figure 4. Electronic circuit for the excitation system.

The op-amp is responsible for shifting the signal down and slightly amplifying it in order to achieve a range of around [−4 V; +4 V]. The selected op-amp for this application is the OPA547T-1G3 from Texas Instruments, which is a high-current output op-amp, and was adapted for this case. The op-amp is in the differential amplifier configuration. In the circuit presented in Figure 4, the resistors were chosen as $\frac{R7}{R6} = \frac{R5}{R4}$ so that $V_{out} = \frac{R7}{R6}(V_{in1} - V_{in2})$. Moreover, R2 = R3 and R8 = R9. The presence of R8 and R9 can be explained by the fact that most of the low-cost ADCs, including the one selected, cannot read negative voltages; the signal read by the ADC in this configuration is, therefore, $\frac{V_{out}+5V}{2}$. The circuit was implemented on a Printed Circuit Board (PCB) in order to simplify the cable management within the device, and the resistors were defined as R1 = R2 = R3 = R4 = R6 = 470 Ω and R5 = R7 = R8 = R9 = 1000 Ω.

The actuators used in this work are the same ones described in Section 2.3, as no design update was necessary for this component.

The generated controlled excitation signal corrected by the custom-devised amplifying and shifting circuit is visible in Figure 5a. In this graph, there is no presence of any voltage irregularity, as observed previously in Figure 3b, before the implementation of the amplifying and shifting circuit. Figure 5b indicates a focus on only four cycles from the same signal visible in Figure 5a, while the sine sweep reaches a frequency of approximately 210 Hz.

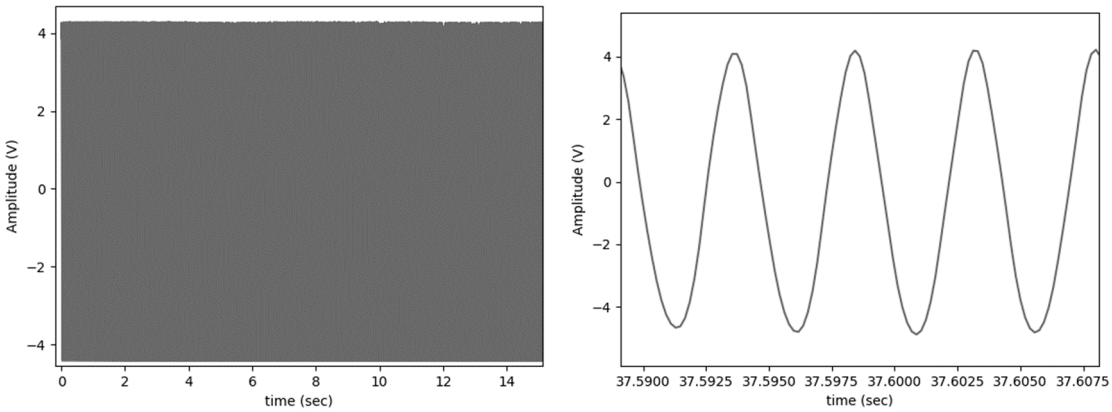

Figure 5. Corrected controlled excitation (**a**) Visualization at 15 s; (**b**) Visualization of four cycles at approximately 210 Hz.

Finally, as several specimens can be monitored in the same experiment (in sequence), the controlled excitation signal passes through a multiplexer, the aim of which is to

distribute the signal to the desired actuator. In the case of the prototype hereby presented, the multiplexer used is in the form of a commercially available relay board that contains four relays.

3.3. Hardware Connections

The proposed system is composed of two sub-systems, the data acquisition system and the controlled excitation system, that have a common central node, namely the RPi. On the one hand, the RPi is connected to the ADC, which is connected to the accelerometers to form the data acquisition system. On the other hand, the RPi is connected to the DAC, which is connected to the amplifying and shifting circuit, itself connected to the multiplexer to which the actuators are connected. Figure 6 shows a schematic representation of the electronic components' interactions discussed in the above sections.

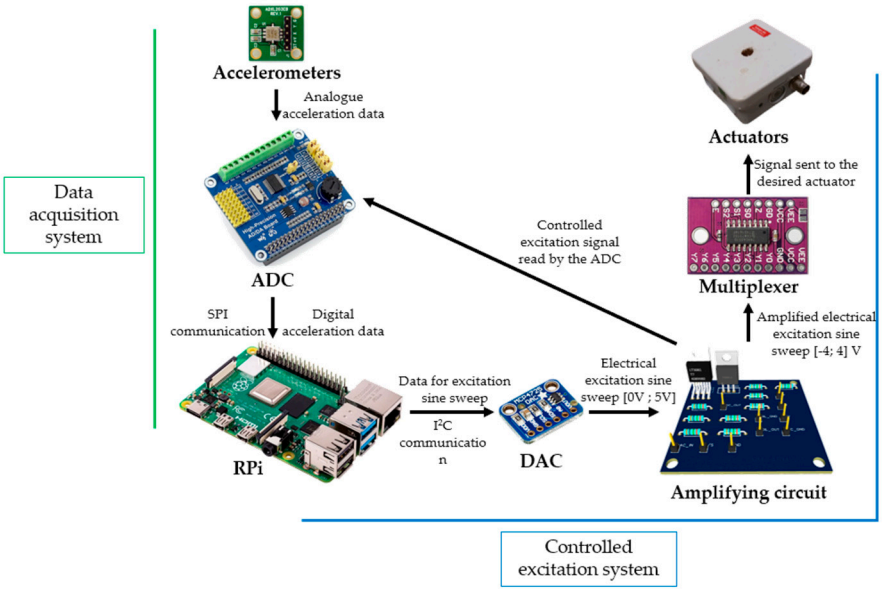

Figure 6. Electronic components interactions.

The wire connections between the different components of the system are visible in Figures 7 and 8. Note that for visualization simplicity purposes, the data acquisition system and the controlled excitation system were represented in two distinct figures. In reality, both systems function in parallel, and the system incorporates a single RPi, as seen in Figure 6. In these figures, the components are represented in a simplified manner as rectangles, with the different I/O connections that they provide, and with the pins named by their suppliers. For the data acquisition system (Figure 7), the RPi powers the ADC and accelerometers via the 5 V supply and ground wires. The RPi communicated with the ADC through the SPI communication protocol, which was made of four wires. The ADC gets the accelerometer's data via a simple wire for each of them. On the other hand, for the controlled excitation system (Figure 8), the RPi powers the DAC and the multiplexer via 5 V supply and ground wires. The RPi communicates with the DAC through the I2C communication protocol, made with two wires. The sine sweep signal generated by the DAC passes by the custom-devised amplifier and the multiplexer before arriving at the actuators. For more clarity in the figure, the external wire connections of the amplifier (+9 V, −9 V, external 5 V and ADC read) were not represented; only the corresponding pins appear on the amplifier's representation. The RPi communicates directly with the multiplexer via three wires with a high/low logic in order to enable or disable the desired output channels.

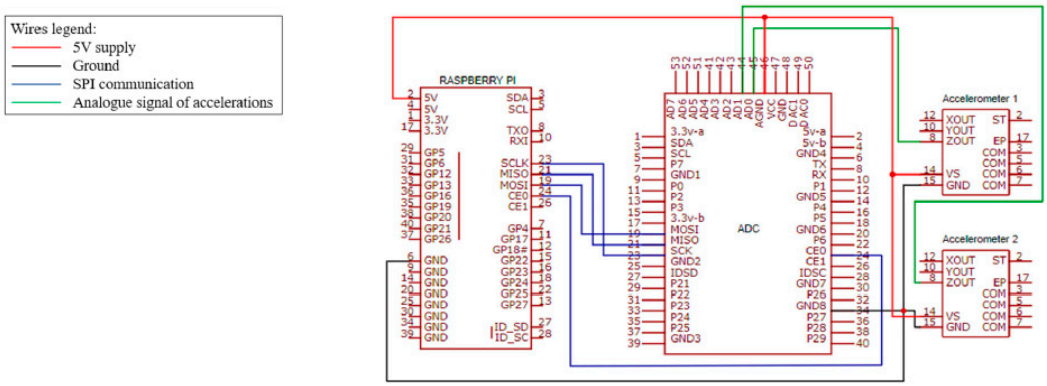

Figure 7. Wire connections in the data acquisition system.

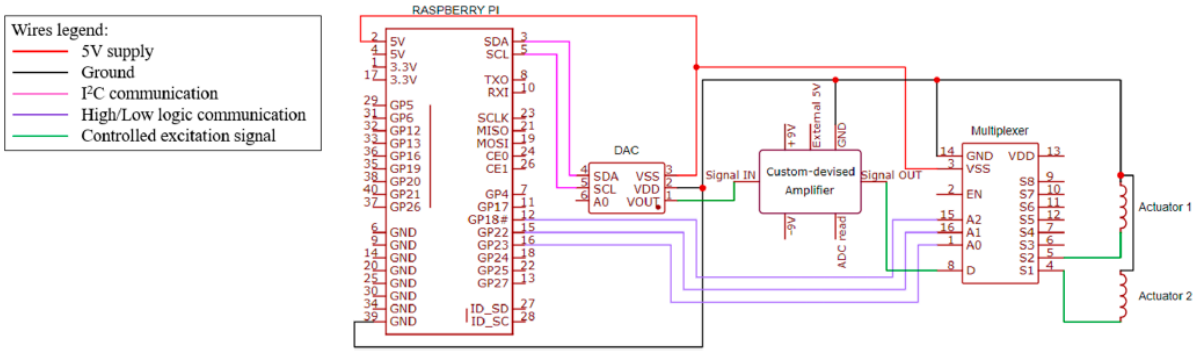

Figure 8. Wire connections in the controlled excitation system.

For portability purposes, the proposed system was integrated into a 3D printed container which is shown in Figure 9. The positioning of the RPi in the assembly can be seen in Figure 9, point 7, and to maintain the clarity of the illustration, no other electronic component is present in this figure, with the exception of the DAC (Figure 9, point 6). To connect the external elements to the system, three different types of connections were used: 3 DC Jack 5.5 × 2.1 mm connectors (Figure 9, point 1) to connect the different power supplies: +9 V, −9 V, and +5 V; BNC connectors to connect the actuators (Figure 9, point 4), and finally SP1310/P3 connectors to connect the accelerometers (Figure 9 point 5). For this prototype, the multiplexer offers four possible connections, which justifies the presence of four connectors of each type. In order to indicate the state of the experiment (which specimen is being monitored, the system waiting for next measurement, etc.) to the user, the system contains four LEDs (Figure 9, point 3). Finally, the proposed system includes a fan (Figure 9, point 2) in order to avoid the overheating of the RPi.

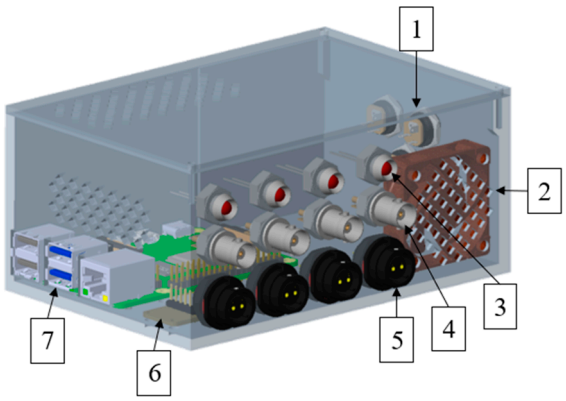

Figure 9. 3D representation of the proposed system's assembly.

The total cost of the proposed EMM-ARM system for applications to two specimens (therefore with two accelerometers) was calculated in December 2022, in Portugal, at a value of EUR 260. The price of the proposed system is therefore approximately one-twentieth the price of the traditional system.

3.4. Software Design

The software aspects of the proposed EMM-ARM system correspond to the algorithm used to conduct the test. The algorithm was coded in the Python programming language, as it is well supported by the RPi, and libraries to interact with the electronic components are available in Python. The algorithm is based on three main parts: the parameter definition, the measurement protocol, and the post-processing part, with the final aim of calculating the E-modulus of the material cast in the mould. In practice, the software is constituted of one main Python code, where the parameters of the experiment can be defined, and five additional Python codes, hosting the functions necessary for the main code's execution. For this prototype's design, no graphical user interface was developed, with the different data calculated (specimens' age, resonant frequencies, E-modulus etc. from the algorithm being printed in the terminal of the Python environment.

The software algorithm can be summarized in the flowchart visible in Figure 10. To interact with the system as proposed in this work, the user needs an external monitor, a mouse, and a keyboard; the RPi, however, offers countless other interaction options, such as web pages, a touch screen, an LCD screen, and push buttons, etc. Once all the parameters required to conduct the tests are given to the algorithm (Figure 10a) and the test is started (Figure 10b), every step is automated, and no more interaction from the user is required. It can be observed that three functions are executed in parallel (Figure 10c): the excitation signal generation, its measurement, and the specimen response vibration measurement. In order to save time and therefore optimize the measurement performances, each measurement is saved in a Python list (Figure 10d) until the measurement duration is reached (Figure 10e), after which the Python lists are saved to CSV files to save the raw data from the experiment (Figure 10f). The post-processing of the data then takes place (Figure 10g) with the modal identification and the E-modulus estimation, which are saved on different CSV files. If more than one specimen is tested (Figure 10h), as previously discussed, their measurement is managed in sequence (with the ADC's sampling frequency limiting the concurrent number of specimens to one); Figure 10i shows that the algorithm switches specimens after the post-processing phase of the data. Once the time between measurements (Figure 10j) is reached, and the experiment remaining time is over (Figure 10k), the test is stopped (Figure 10l).

In order to achieve the simultaneous execution of the tasks for the controlled excitation and the measuring of it together with the response vibration (Figure 10c), a parallel processing technique was used, namely multiprocessing. Multiprocessing is a method of concurrent execution in which multiple processes are executed simultaneously in order to increase the overall performance and efficiency of a system [41]. Each process runs independently of one another and has its own memory space, making it an effective way to utilise multiple processing cores [42]. A process can be defined as an instance of a program that is being executed. It is a self-contained execution environment that consists of a set of instructions, a program counter, and a memory space. Each process is given a unique process identifier which allows the operating system to track and manage it [43]. In multiprocessing, a parent process will spawn child processes, which will run concurrently with the parent process. These child processes can communicate with the parent process and with each other through various inter-process communication mechanisms such as pipes, shared memory, and message queues [44]. On low-cost computing devices such as the RPi, few references can be found in the literature with regard to the use of multiprocessing techniques, although the RPi is adapted for multiprocessing, as the CPU integrates four cores.

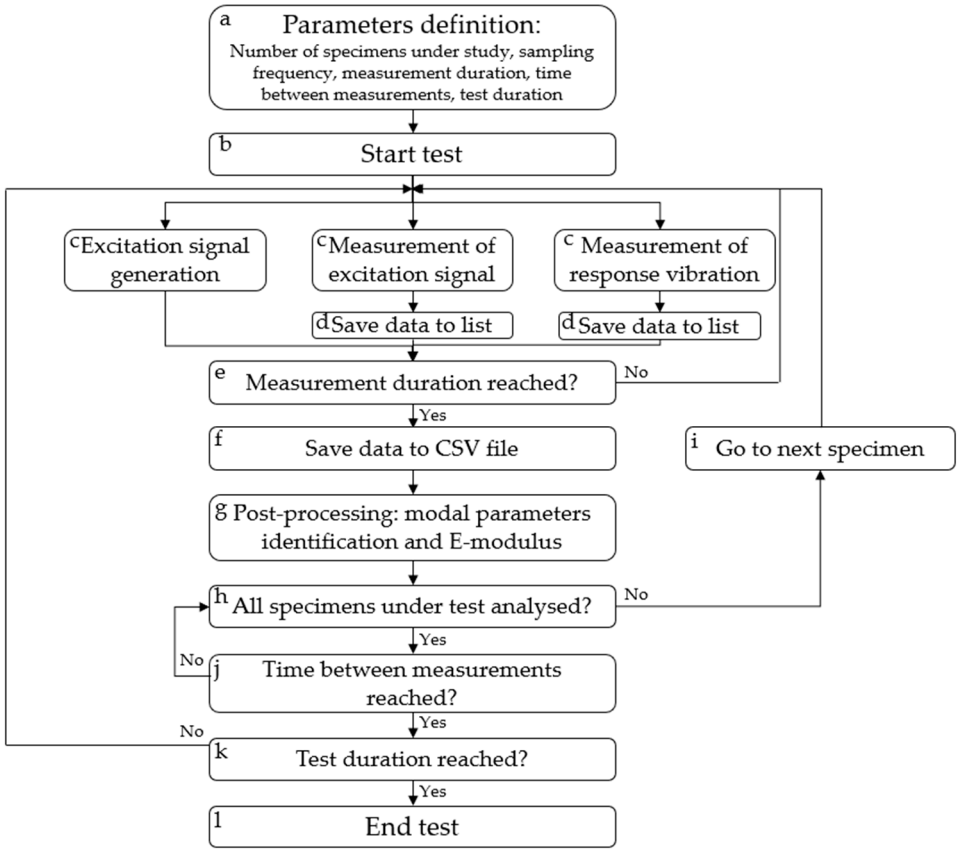

Figure 10. Algorithm flowchart.

It is important to note that multiprocessing must be differentiated from multithreading, which is a popular programming technique that is more lightweight than multiprocessing. Threads are the smallest units of execution that can be scheduled by the operating system [45]. Multithreading is a technique that allows a single process to have multiple threads of execution. Each thread has its own program counter, stack, and local variables, but shares the same memory space as the other threads within the same process [46]. This allows for the concurrent execution of multiple parts of a program, (threads) within a single process, for compatible devices and compatible programming environments. A key parameter to consider before using the multithreading programming technique in a Python environment is the Global Interpreter Locker (GIL). The GIL is a mechanism used in the Python programming language to ensure the sequential execution of threads within a single process. This lock was implemented to safeguard the access to the resources of the Python interpreter and allow only one thread at a time to acquire the lock. This approach improves the efficiency of single-core environments, as the GIL can be temporarily unlocked when a thread is waiting for an I/O operation, thereby enabling time slicing techniques to optimize the performance [46]. Consequently, the GIL can limit the performance benefits of multi-threaded programs on multi-core systems, as only one thread can run at a time. However, the GIL is still essential for ensuring the correct behaviour of multi-threaded Python programs. Even though the operating system's scheduler can switch between threads, allowing multiple threads to be executed in a time-shared manner on a single core, the performances reached are often over classed by the multiprocessing ones.

The multiprocessing Python library offers the possibility to bypass the bottleneck induced by the GIL, at the cost of computing power, by creating various processes, each possessing its own Python interpreter [47].

As the computing power is not a limiting factor for the RPi in an EMM-ARM experiment, the multiprocessing technique was used to achieve the concurrent execution

of the controlled excitation function and the measurements' function. In practice, the function responsible for generating the excitation signal is managed by one process, while the measurement function is managed by another process simultaneously, allowing these two functions to be executed in parallel on two distinct CPU cores.

Once the raw data are collected, they need to be post-processed, as illustrated in Figure 10g. This post-processing phase was directly implemented in the developed system to monitor the E-modulus evolution in real-time, after each phase of monitoring. A detrend filter (linear type) is firstly applied to the raw data in order to remove any linear derivation that could occur throughout the experiment. A bandpass filter (order: 8; frequencies: [10;250] Hz) is then applied to maintain the relevant frequency range.

The modal parameters identification method used in the presented research is the same as the one used in the traditional EMM-ARM system, namely the SSI method. However, the implemented variant was adapted from [48], which is an application for OMA experiments. The complete Python code of the implemented method is available in [49]. The modal identification consists in building a model with different orders and verifying the stability of the eigenfrequencies, damping ratios and modal shapes from one order to another. The combination of the three parameters, eigenfrequency, damping ratio and modal shape constitutes a pole; when iterating the analysis on the different model orders, the stable poles are counted to identify the vibration modes. In the EMM-ARM application, only the first resonant frequency of the specimen under testing is located in the frequency range of measurement (due to the different properties of the specimen); therefore, the mode identified by the SSI program corresponds to the first resonant frequency of the specimen. More details regarding the analysis procedure can be found in [48].

Even though this variant is adapted for OMA, it was implemented in this research to analyse data from both cement paste tests (environmental excitation) and mortar tests (controlled excitation). The data from the excitation signal, for concrete and mortar tests, are then analysed to verify that their normalized power spectrum density is constant over the duration of the experiment, which ensures that all frequencies were excited with the same intensity, to verify the applicability of the SSI method.

4. Experimental Validation

The overall experimental validation strategy consisted of three experiments: the first one was conducted on one cement paste specimen, which began minutes after casting and lasted for 13 days and was designed to assess the ability of the proposed system to reliably measure low-amplitude vibrations without generating the controlled excitation. The second experiment was conducted on two hardened mortar specimens to verify the capacity of the proposed system to manage experiments with more than one specimen and to generate the controlled excitation while monitoring the specimens' vibrations. Finally, the third experiment, considered as a full validation experiment, involved the monitoring of two mortar specimens from minutes after casting for a total of 7 days. For each of the tests, the results obtained with the proposed system were compared to those obtained with the traditional EMM-ARM system, which was thoroughly validated and compared to other methods to characterize the E-modulus of cement-based materials in [18]; therefore, the specimens were equipped with accelerometers from both systems.

4.1. Materials

The material used for the first experiment on hardening cement paste was a cement CEM II/B-L 32.5 from Secil. A ratio of 0.5 for water/cement was considered, in mass, to achieve a good consistency for moulding the specimens without the need to use a superplasticizer. The mixing procedure was made following the EN 196-3 standard. The mould was filled manually, and no compaction was performed.

For the second experiment on hardened mortar specimens, since the aim was simply to compare the identified resonant frequencies between the two systems, random available mortar samples were taken from previous unidentified research conducted on the

E-modulus measurement of mortars with the EMM-ARM. Thus, no data regarding the type of mortar used is available for these specimens.

Regarding the third experiment on hardening mortar specimens, a ready-mix mortar from Secil, the Redur Multi, which is a M10 mortar, was used. The ready-mix mortar was mixed with water in the proportions indicated by the supplier: 3 L of water per bag of 25 kg. The datasheet of the mortar can be found in [50]. The mixing procedure was made following the standard EN 196-3. The moulds were filled manually, and compaction of the material in the moulds was performed on a compaction table (50 Hz) according to the standard EN 12390-1.

4.2. Methods

For the first experiment, the cement paste specimen was in cantilever conditions and was excited by the airflow of a fan placed in the vicinity, as shown in Figure 11. In this figure, the numbering corresponds to: (1) data acquisition from the traditional system, (2) the laptop for the traditional system, (3) a fan, (4) an accelerometer from the traditional system, attached to the specimen with hot glue, (5) an accelerometer from the proposed system, attached to the specimen with hot glue, (6) the proposed system, (7) a clamping device, and (8) a specimen. The mould and setup (clamping device) used in this experiment conformed to those used in previous studies on the EMM-ARM application to cement paste [18]. The specimen's vibrations were measured by both systems, the traditional one and the proposed one. The information regarding the mould properties as well as the configuration of the traditional and proposed systems are presented in Table 2. Furthermore, only the frequency evolution of the hardening specimen was analysed, as the aim of the test was to assess whether the developed system could satisfactorily estimate frequencies from low-amplitude ambient response tests.

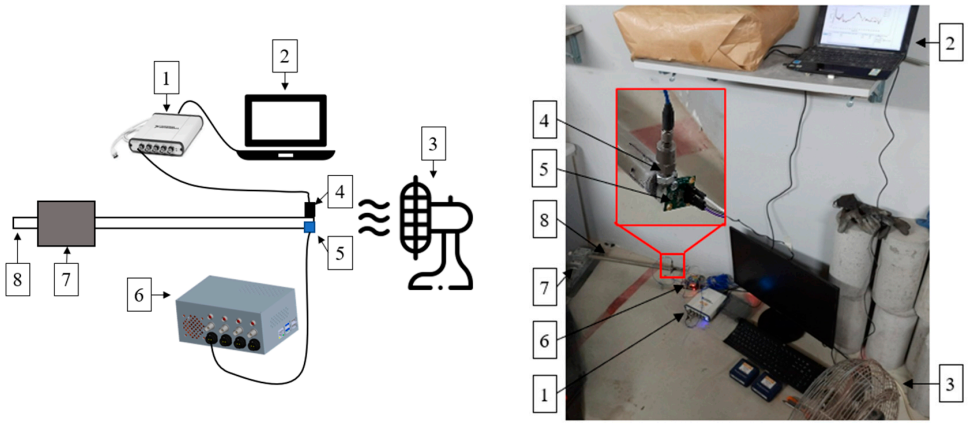

Figure 11. Experimental setup for cement paste test: (**a**) schematic representation; (**b**) a picture of the experiment.

Table 2. First experiment information.

Specimen Information		Systems Configuration	
$Ø_i$	16.63 mm	Measurement time	600 s
$Ø_e$	20.14 mm	Time between measurements	600 s
Total length	550 mm	Sampling frequency	
Span	450 mm	Traditional system	1000 Hz
Mould material	Acrylic	Proposed system	1000 Hz
Mould stiffness	4.03 GPa		
Mould mass	67.4 g		
Total mass	286.32 g		

For the second experiment on hardened mortar specimens, as existing unspecified specimens were taken from previous research, only data that could be measured on the hardened specimens can be proposed. The specimens were in simply supported conditions, and the setup (supports) conformed to those used in previous research on EMM-ARM applications to mortars [19]. The experimental setup for this test can be visualized in Figure 12. In this figure, the numbering corresponds to: (1) a laptop for the traditional system, (2) the proposed system, (3) the accelerometer from the proposed system, attached to the specimen with hot glue, (4) actuators, (5) supports, (6) a specimen, (7) an accelerometer from the traditional system, attached to the specimen with hot glue, and (8) data acquired from the traditional system. Note that for clarity purposes, only one of the two specimens was represented in the schematic of Figure 12a. but both specimens were connected to the two systems in the same way. The controlled excitation was generated by the proposed system, while both systems, the traditional and the proposed one, measured the specimens' vibrations. The measurement consisted in 7 repetitions of 600 s long data acquisition sessions. Hence, this experiment aims as comparing punctual results obtained from both systems, rather than comparing average values like operated on the longer-term experiments 1 and 3. The analysis consisted in comparing the frequency estimations performed in the specimens with each system and assessing the repeatability of such estimations. The available information regarding the specimens used in this experiment, as well as the configuration of the traditional and proposed systems are presented in Table 3.

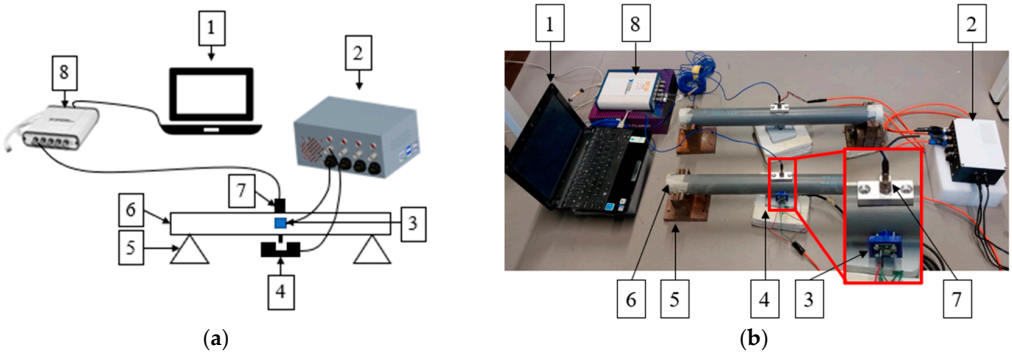

Figure 12. Experimental setup for the mortar test: (**a**) schematic representation; (**b**) a picture of the experiment.

Table 3. Second experiment information.

	Specimen 1	**Specimen 2**	**Systems Configuration**	
$Ø_e$	50.2 mm	50.1 mm	Measurement time	600 s
Total length	551 mm	552 mm	Sampling frequency	
Span	500 mm	500 mm	Traditional system	1000 Hz
Material	PVC	PVC	Proposed system	1000 Hz
Total mass	1845.2 g	1844.4 g		

Regarding the third experiment, the mortar specimens were in simply supported conditions, and the moulds used, as well as the setup (supports), conformed to those used in previous studies on the EMM-ARM application to mortars [19]. The setup of this experiment was identical to the one presented in Figure 12. The controlled excitation was generated by the proposed system for the two specimens, while both systems, the traditional and the proposed one, were measuring the specimens' vibrations. The information regarding the mould properties as well as the configuration of the traditional and proposed systems are presented in Table 4. As the two specimens' vibrations were measured in sequence, the time between measurements corresponds to the time between two consecutive measurement sessions on the same specimen; this duration was determined in order to

obtain two measurement sessions of each specimen per hour. During the experiment, the resonant frequencies of the two composite beams composed of the material in their moulds were identified, and used, together with the different values presented in Table 4, in order to calculate the tested material's E-modulus.

Table 4. Information on the third experiment.

	Specimen 1	Specimen 2	Systems Configuration	
$Ø_i$	44.2 mm	44.55 mm	Measurement time	600 s
$Ø_e$	50.2 mm	50.3 mm	Time between measurements	1800 s
Total length	549 mm	551 mm	Sampling frequency	
Span	500 mm	500 mm	Traditional system	1000 Hz
Mould material	PVC	PVC	Proposed system	1000 Hz
Mould Stiffness	3.5 GPa	3.1 GPa		
Mould mass	358.71 g	332.74 g		
Total mass	2033.9 g	2055.5 g		

4.3. Results and Discussion

The results of the first experiment conducted on a hardening cement paste specimen are presented in Figure 13. The graph in Figure 13a represents the evolution of the resonant frequency of the specimen through time, with each point corresponding to a frequency estimation obtained from a measurement session. The graph in Figure 13b represents the moving average (parameter: 20 values) of the frequency evolution measured by both systems. A clear and consistent superposition of the curves obtained by both systems can be observed on these graphs. For the accuracy estimation of the proposed system during this experiment, the average absolute difference, throughout all ages of the entire experiment between the two systems was calculated, and was determined to be 0.7%. This allows us to safely conclude that the proposed system reaches performances sufficient for continuously measuring the E-modulus of cement paste specimens. In order to control the measurement quality of the proposed system, and to compare it with the traditional system's one, as well as to verify that no quality degradation occurred throughout the experiment, the stabilization diagrams obtained at the beginning and at the end of the experiment are represented in Figure 14. The stabilization diagrams were obtained from the SSI method, and show the stable poles for the different model orders, plotted on the NPSDs. In this figure, the measurement quality of both systems appears to be highly comparable, with an ideal identification of the peak corresponding to the resonant frequency of the specimen. This figure highlights the reliability of the proposed system measurements, as the stabilization diagrams present no noticeable disturbance.

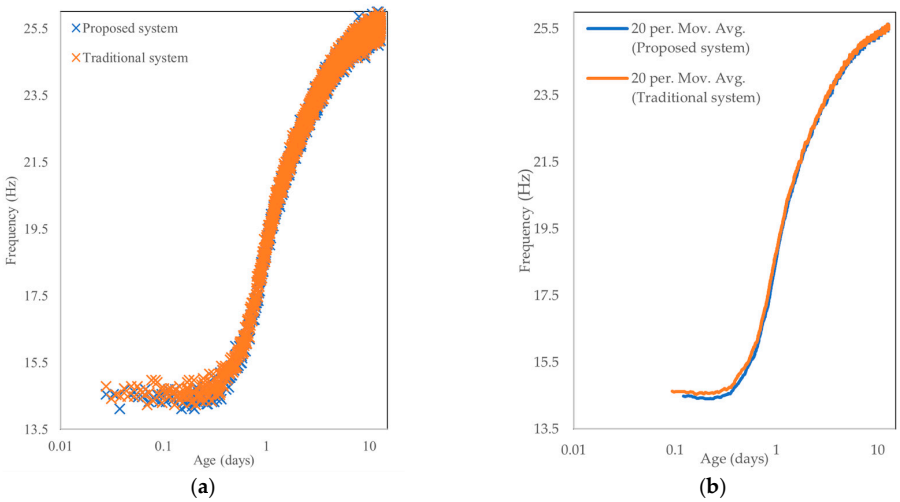

Figure 13. Cement paste test graphs of (**a**) frequency curve; (**b**) moving average.

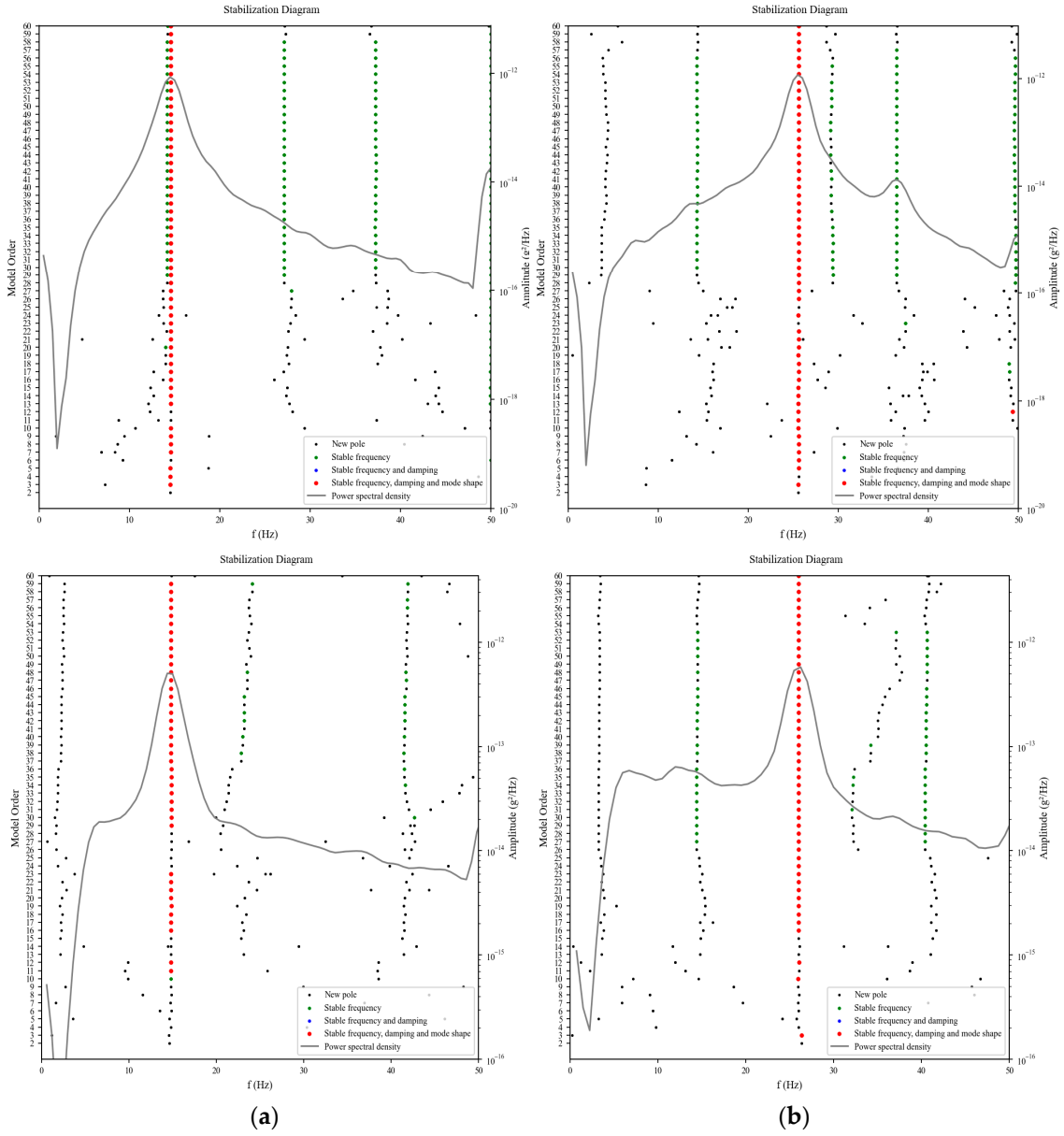

Figure 14. Stabilization diagrams at different ages (the top one corresponds to the traditional system, while the bottom one corresponds to the proposed system); (**a**) 0 days; (**b**) 13 days.

This experiment assessed the ability of the developed system to identify accelerations at relatively low frequencies compared to those obtained in mortar experiments.

The results obtained from the second experiment, conducted on hardened mortar specimens, are presented in Table 5. The NPSDs of the controlled excitation signals were observed as constant over the frequency range of excitation [20;250] Hz, as illustrated in Figure 15, which allows the application of the modal identification method (less than 2% of absolute difference between the amplitudes at 20 Hz and 250 Hz). During this test, the resonant frequencies of the two specimens were identified with both the traditional and proposed systems. The proposed system presents results less than 1% different from those of the traditional one. With regard to the standard deviation between each measurement, the proposed system shows slightly higher values than the traditional system, but is still in the same range. To illustrate the measurement and modal identification quality in this experiment, the stabilization diagrams of the first run for the specimen 1 obtained with both systems are represented in Figure 16. The graphs in this figure exhibit a single predominant peak which corresponds to the resonant frequency of the specimen; narrow peaks are

visible, at 100 Hz and 50 Hz, respectively, for the traditional and the proposed systems, corresponding to electrical noise. Electrical noise is present in any electronic system and is usually observed as peaks at 50 Hz and harmonics on the multiples of 50 Hz on NPSDs [51]. On these graphs, the proposed system clearly suffers from a higher intensity of the measured electrical noise. The traditional system, using specialized equipment, appears to be much more performant than the proposed system for reducing the electrical noise (isolation of cables and connectors, anti-aliasing filters etc.). Despite the presence of electrical noise, the SSI method's performance is highlighted in Figure 16, as only the predominant peak is identified as the resonant frequency.

Table 5. Test results of the hardened mortar specimens.

Traditional System									
Frequency (Hz)	Run 1	Run 2	Run 3	Run 4	Run 5	Run 6	Run 7	Average	Standard deviation
Specimen 1	162.8	161.8	162.6	161.4	162.4	162.6	162.9	162.4	0.55
Specimen 2	92.1	93.2	93.5	92.2	92.8	92.5	92.9	92.7	0.51
Proposed system									
Specimen 1	161.8	161.2	161.4	161.8	162.6	162.4	163.4	162.1	0.76
Difference (%)	0.61	0.37	0.74	0.25	0.12	0.12	0.31	0.36	
Specimen 2	92.3	93.1	91.9	91.8	92.1	91.7	91.7	92.1	0.50
Difference (%)	0.22	0.11	1.71	0.43	0.75	0.86	1.29	0.88	

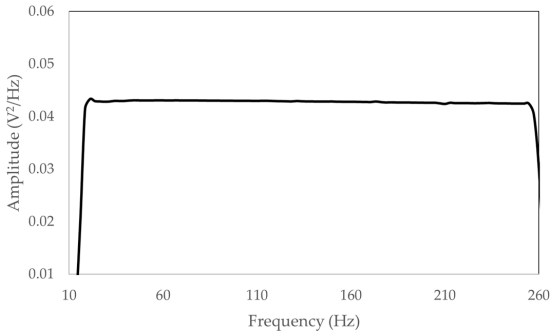

Figure 15. NPSD of the controlled excitation of the second run on specimen 1.

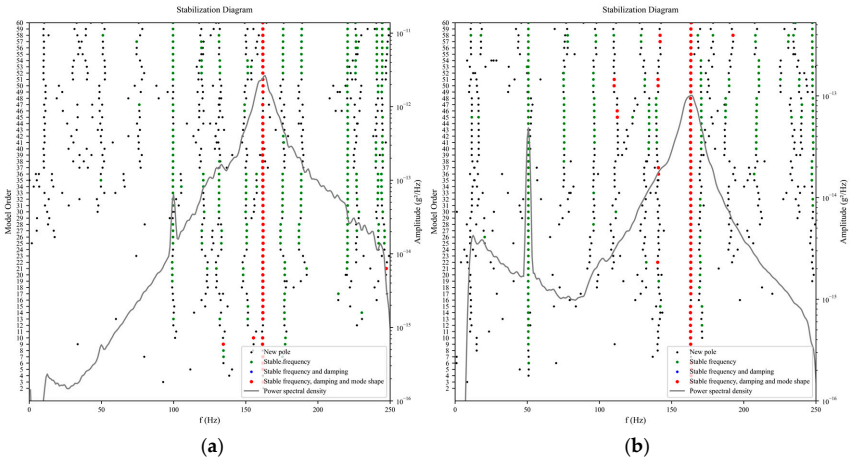

(**a**) (**b**)

Figure 16. Stabilization diagrams obtained with (**a**) the traditional system; and (**b**) the proposed system.

Considering these results, it is safe to conclude that the proposed system is adequate for measuring the E-modulus of hardened mortar specimens with controlled excitation. This test assessed the ability of the developed system to identify frequencies substantially

higher than those obtained with cement paste specimens. It also evaluated the ability of the proposed system to generate the controlled excitation while monitoring the vibration response of the specimens.

Finally, regarding the third validation experiment, as it spanned over a significantly longer time than the second experiment, it is firstly necessary to verify that the controlled excitation generated by the proposed system presents constant values on its NPSD over the range of excitation ([20; 250] Hz) during the whole experiment. The controlled excitation NPSD over the full duration of the experiment can be seen in Figure 17. As can be observed in this figure, the NPSD can be approximated as constant over the range of frequencies; less than 8% of absolute difference between the amplitudes at 20 Hz and 250 Hz were measured. From an engineering perspective, these values are similar enough to consider that the excitation is of the same order over the frequency range.

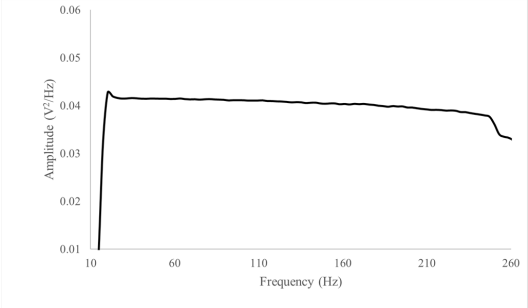

Figure 17. The NPSD of the controlled excitation signal over the full duration of the experiment.

Due to concurrent experiments in the laboratory as well as to power failure, the measurements were interrupted twice: a 14-h monitoring break was applied after 2 days of monitoring, and a 2 day monitoring break was applied on days 5 and 6 of the experiment.

The results obtained on the third experiment showed consistency between the measurements from the traditional and proposed systems. Figure 18a represents the evolution of the identified first resonant frequency of the specimens during the test. For the same specimen, the superposition of the points obtained from the two systems highlights the reliability of the measurements from the developed system. For the accuracy estimation of the proposed system during this experiment, the average absolute differences, throughout all ages of the entire experiment, between the frequencies obtained from the two systems, were calculated, and measured 1.1% and 1.5%, for specimen 1 and specimen 2, respectively. These levels of accuracy assess the measurement reliability of the proposed system.

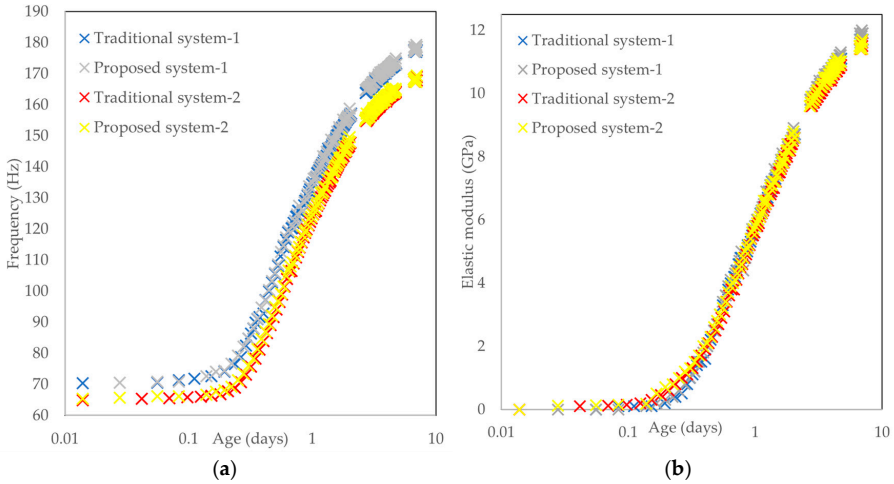

Figure 18. Hardening mortar test graphs of (**a**) frequency curves; and (**b**) elastic modulus curves.

A considerable difference in terms of frequency that was measured by both systems was noticed between the two specimens. The average absolute difference between the measurements of the two specimens by the traditional system was calculated to be 6.3%. This difference is explained by the specimens' properties, which were mainly influenced by the combination of a slightly stiffer mould and lighter mass for specimen 1, which translates to higher vibration frequencies, as seen in Figure 18a.

The E-modulus evolution of the two specimens presented in Figure 18b confirms these observations, since the E-modulus evolution curves exhibit comparable values between the two specimens. Over the experiment's duration, the E-modulus estimations, independently from the systems and specimens, remain, on average, within a range of ± 0.36 GPa, which indicates the reliability of the proposed system.

In order to further analyse the measurement quality of the proposed system, and to verify that no degradation occurred throughout the duration of the experiment, stabilization diagrams obtained at the beginning and at the end of the experiment are presented in Figure 19. In this figure, the electrical noise measured by the proposed system appears to be of high intensity (narrow peak at 50 Hz), but was not identified as a resonant frequency by the SSI method. The peak corresponding to the resonant frequency of the specimen is predominant in each graph, and is correctly identified by the SSI method. This figure reveals the main advantage of using specialized equipment for the EMM-ARM applications, as only neglectable electrical noise is measured by the traditional system, even though its presence in the measurements from the proposed system does not affect the experiment results.

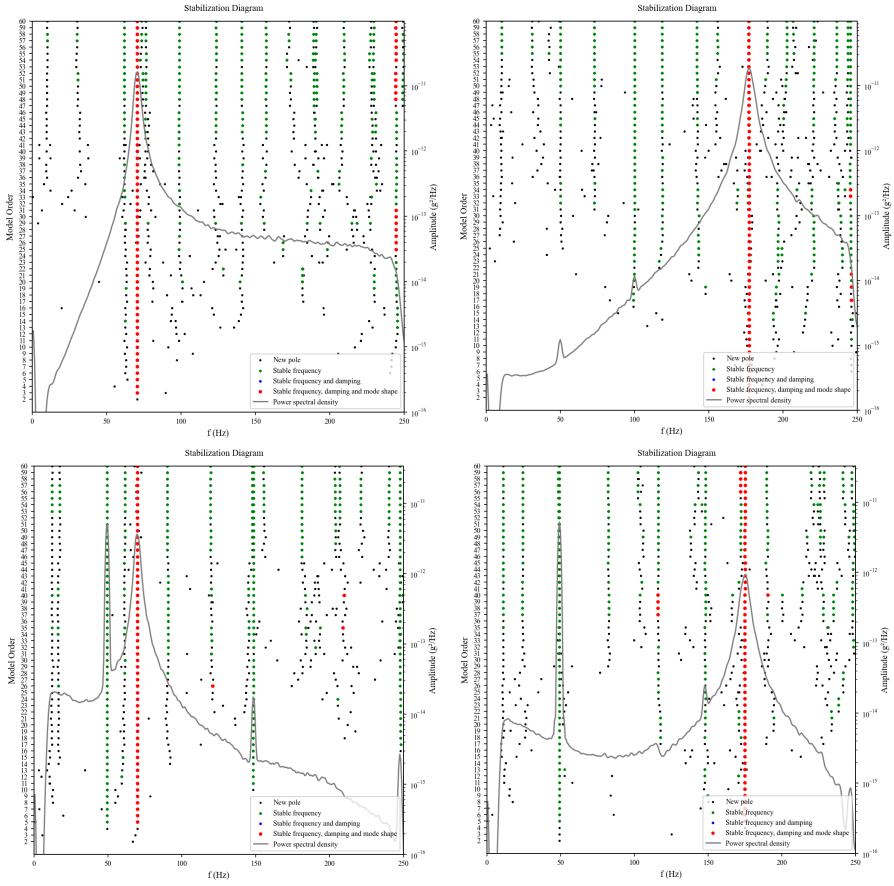

Figure 19. Stabilization diagrams at different ages (the top corresponds to the traditional system, while the bottom diagram corresponds to the proposed system); (**a**) 0 days; (**b**) 7 days.

5. Conclusions

In this study, a new system capable of performing EMM-ARM tests on cement paste and mortar specimens was presented. The system was designed using cost-effective components and open-source resources, with the aim of increasing its dissemination and scalability in various use cases. Compared to traditional systems, the proposed system was found to be significantly less expensive (20 times lower), without factoring in the cost of software licenses.

Despite using cost-effective electronic components, the results obtained from the experiments provide evidence for the proposed EMM-ARM system's feasibility as a monitoring tool for the early-age E-modulus evolution of cement paste and mortar applications. Regardless of the experiment type, whether cement paste with ambient vibration excitation or mortar applications with a controlled excitation, the proposed system demonstrated reliable measurement abilities.

The proposed system consistently produced comparable results to those obtained with the traditional system in all experiments conducted. This suggests that the traditional system may use over-designed components for the intended application. Additionally, the obtained results are seen as representative enough to demonstrate the viability of the system for all the materials already tested with EMM-ARM in the past (e.g., epoxy, soil cement, cement paste, mortar, and concrete), as the range of frequencies and excitability of the specimens fall in similar ranges to the ones tested here.

To promote the dissemination of the proposed system, the system design and codes will be made available on the GitHub platform through the link available in [17], and it is freely available for anyone to use according to the MIT License. This will allow other interested parties in academia or in industry to benefit from this work.

The presented work's impact can be significant in light of the possibility to be implemented in various laboratories as well as in an industrial environment, with a strong potential to democratize access to advanced characterisation techniques such as the EMM-ARM, in addition to many others.

Author Contributions: Conceptualization, T.R., R.R.R., R.d.M.L., J.G. and M.A.; methodology, T.R., J.G. and M.A.; software, T.R. and R.R.R.; validation, T.R., J.G. and M.A.; format analysis, T.R.; investigation, T.R., R.R.R., A.A., R.d.M.L., J.G. and M.A.; resources, T.R.; data curation, T.R., writing—original draft preparation, T.R., J.G. and M.A.; writing—review and editing, T.R., R.R.R., A.A., R.d.M.L., J.G. and M.A.; visualization, T.R.; supervision, J.G. and M.A.; project administration, J.G. and M.A.; funding acquisition, Miguel Azenha. All authors have read and agreed to the published version of the manuscript.

Funding: This work was partly financed by FCT/MCTES through national funds (PIDDAC) under the R&D unit of the Institute for Sustainability and Innovation in Structural Engineering (ISISE), under reference UIDB/04029/2020, and under the Associate Laboratory Advanced Production and Intelligent Systems (ARISE) under reference LA/P/0112/2020. This project has received funding from the European Union's Horizon 2020 research and innovation programme under the Marie Sklodowska-Curie project SUBLime [Grant Agreement n. 955986].

Data Availability Statement: All data obtained throughout the experiments conducted in the framework of this paper are available from the corresponding author by official request.

Conflicts of Interest: The authors declare no conflict of interest.

References

1. Boumiz, A.; Vernet, C.; Cohen Tenoudji, F. Mechanical Properties of Cement Pastes and Mortars at Early Ages. *Adv. Cem. Based Mater.* **1996**, *3*, 94–106. [CrossRef]
2. Chawla, K.K.; Meyers, M.A. *Mechanical Behavior of Materials*; Cambridge university press: Cambridge, UK, 2008.
3. Chen, Y.; Liu, P.; Sha, F.; He, S.; Lu, G.; Yu, Z.; Chen, H. Preparation and Performance of the Ultra-High Performance Mortar Based on Simplex-Centroid Design Method. *J. Mater. Res. Technol.* **2021**, *15*, 3060–3077. [CrossRef]
4. Cui, K.; Liang, K.; Chang, J.; Lau, D. Investigation of the Macro Performance, Mechanism, and Durability of Multiscale Steel Fiber Reinforced Low-Carbon Ecological UHPC. *Constr. Build. Mater.* **2022**, *327*, 126921. [CrossRef]

5. Cui, K.; Chang, J. Hydration, Reinforcing Mechanism, and Macro Performance of Multi-Layer Graphene-Modified Cement Composites. *J. Build. Eng.* **2022**, *57*, 104880. [CrossRef]
6. Azenha, M.; Magalhães, F.; Faria, R.; Cunha, Á. Measurement of Concrete E-Modulus Evolution since Casting: A Novel Method Based on Ambient Vibration. *Cem. Concr. Res.* **2010**, *40*, 1096–1105. [CrossRef]
7. Braun, S. Signal Processing, Model Based Method. In *Encyclopedia of Vibration*; Braun, S., Ed.; Elsevier: Oxford, UK, 2001; pp. 1199–1208, ISBN 978-0-12-227085-7.
8. Bird, J.O.; Chivers, P.J. 36-Simply Supported Beams. In *Newnes Engineering and Physical Science Pocket Book*; Bird, J.O., Chivers, P.J., Eds.; Newnes: Oxford, UK, 1993; pp. 278–286, ISBN 978-0-7506-1683-6.
9. Granja, J.; Azenha, M. Continuous Monitoring of Concrete Mechanical Properties since an Early Age to Support Construction Phasing. In Proceedings of the CONCREEP 10, Vienna, Austria, 21–23 September 2015; American Society of Civil Engineers: Reston, VA, USA; pp. 1360–1370.
10. Azenha, M.; Ferreira, C.; Silva, J.; Correia, A.; Aguilar, R.; Ramos, L. Continuous Stiffness Monitoring of Cemented Sand through Resonant Frequency. *Geotech. Spec. Publ.* **2011**, *218*, 174–183. [CrossRef]
11. Luís Granja, J.; Azenha, M.; De, C.; Civitest, S.; Maria, C.; Ferreira, F.; Granja, J.L.; de Sousa, C.; Ferreira, C.; Matsuda, T.; et al. Comparison between Different Experimental Techniques for StiffnessMonitoring of Cement Pastes. *J. Adv. Concr. Technol.* **2014**, *12*, 46–61. [CrossRef]
12. Rocha Ribeiro, R.; Sousa, M.I.C.; Rêgo, J.H.d.S.; Lameiras, R.D.M. Innovative Low-Cost System for Early Age E-Modulus Monitoring of Cement Pastes: Validation and Application to Nanosilica-Added and Limestone-Calcined Clay Cements. *Mater. Struct. Mater. Constr.* **2022**, *55*, 13. [CrossRef]
13. Texas Instruments ADS111x Ultra-Small, Low-Power, I2C-Compatible, 860-SPS, 16-Bit ADCs with Internal Reference, Oscillator, and Programmable Comparator. Available online: https://www.ti.com/lit/ds/symlink/ads1115.pdf (accessed on 23 November 2022).
14. Analog Devices ADXL335. Available online: https://www.sparkfun.com/datasheets/Components/SMD/adxl335.pdf (accessed on 14 September 2022).
15. Engard, N.C. 2-Community and Open Source. In *Practical Open Source Software for Libraries*; Engard, N.C., Ed.; Chandos Publishing: Cambridge, UK, 2010; pp. 13–21, ISBN 978-1-84334-585-5.
16. Lahti, C.B.; Peterson, R. (Eds.) Chapter 4-Why Open Source? In *Sarbanes-Oxley IT Compliance Using COBIT and Open Source Tools*; Syngress: Burlington, NJ, USA, 2005; pp. 81–110, ISBN 978-1-59749-036-8.
17. Russo, T.; Ribeiro, R.R.; Granja, J.; Azenha, M. GitHub: Cost-Effective EMM-ARM. Available online: https://github.com/ThomasRusso1/Cost-effective-EMM-ARM (accessed on 24 February 2023).
18. Granja, L.J.D. Continuous Characterization of Stiffness of Cement-Based Materials: Experimental Analysis and Micro-Mechanics Modelling. Ph.D. Thesis, Universidade do Minho Escola de Engenharia, Braga/Guimarães, Portugal, 2016.
19. Ramesh, M.; Azenha, M.; Lourenço, P.B. Study of Early Age Stiffness Development in Lime–Cement Blended Mortars. In *RILEM Bookseries*; Springer: Dordrecht, The Netherlands, 2019; Volume 18, pp. 397–404.
20. Silva, J.; Azenha, M.; Correia, A.G.; Granja, J. Continuous Monitoring of Sand-Cement Stiffness Starting from Layer Compaction with a Resonant Frequency-Based Method: Issues on Mould Geometry and Sampling. *Soils Found.* **2014**, *54*, 56–66. [CrossRef]
21. Azenha, M.; Faria, R.; Magalhães, F.; Ramos, L.; Cunha, Á. Measurement of the E-Modulus of Cement Pastes and Mortars since Casting, Using a Vibration Based Technique. *Mater. Struct. Mater. Constr.* **2012**, *45*, 81–92. [CrossRef]
22. Benedetti, A.; Fernandes, P.; Luís Granja, J.; Azenha, M. Effects of Curing Temperature on Pull-out Behavior and Stiffness Evolution of Epoxy Adhesives for NSM-FRP Applications. In Proceedings of the SMAR 2015, Antalya, Turkey, 7–9 September 2015.
23. Grocel, J. Comparison of Deterministic and Stochastic Method in Operational Modal Analysis in Application for Civil Engineering Structures. *Procedia Eng.* **2014**, *91*, 130–135. [CrossRef]
24. Azenha, M.; Silva, J.; Granja, J.; Gomes-Correia, A. A Retrospective View of EMM-ARM: Application to Quality Control in Soil-Improvement and Complementary Developments. *Procedia Eng.* **2016**, *143*, 339–346. [CrossRef]
25. He, J.; Fu, Z.-F. 8-Modal Analysis Methods—Frequency Domain. In *Modal Analysis*; He, J., Fu, Z.-F., Eds.; Butterworth-Heinemann: Oxford, UK, 2001; pp. 159–179, ISBN 978-0-7506-5079-3.
26. PCB Piezotronics. Available online: https://www.pcbpiezotronics.fr/produit/accelerometre/tld352c34/ (accessed on 24 February 2023).
27. National Instruments. Available online: https://www.ni.com/docs/en-US/bundle/usb-443x-seri/resource/372485e.pdf (accessed on 24 February 2023).
28. Welch, P. The Use of Fast Fourier Transform for the Estimation of Power Spectra: A Method Based on Time Averaging over Short, Modified Periodograms. *IEEE Trans. Audio Electroacoust.* **1967**, *15*, 70–73. [CrossRef]
29. Azenha, M.; Ramos, L.F.; Aguilar, R.; Granja, J.L. Continuous Monitoring of Concrete E-Modulus since Casting Based on Modal Identification: A Case Study for in Situ Application. *Cem. Concr. Compos.* **2012**, *34*, 881–890. [CrossRef]
30. Ramesh, M.; Azenha, M.; Lourenço, P.B. Mechanical Properties of Lime-Cement Masonry Mortars in Their Early Ages. *Mater. Struct.* **2019**, *52*, 13. [CrossRef]
31. Peeters, B. System Identification and Damage Detection in Civil Engineering. Ph.D. Thesis, Katholieke Universiteit Leuven, Leuven, Belgium, 2000.

32. Peeters, B.; Roeck, G. De Stochastic System Identification for Operational Modal Analysis: A Review. Journal of Dynamic Systems, Measurement and Control, Transactions of the ASME. *J. Dyn. Syst. Meas. Control* **2001**, *123*, 659–667. [CrossRef]
33. Peeters, B.; de Roeck, G. Reference-Based Stochastic Subspace Identification for Output-Only Modal Analysis. *Mech. Syst. Signal. Process* **1999**, *13*, 855–878. [CrossRef]
34. Deraemaeker, A.; Reynders, E.; de Roeck, G.; Kullaa, J. Vibration-Based Structural Health Monitoring Using Output-Only Measurements under Changing Environment. *Mech. Syst. Signal Process* **2008**, *22*, 34–56. [CrossRef]
35. Raspberry Pi Raspberry Pi 4 Computer Model B. Available online: www.raspberrypi.org (accessed on 12 April 2023).
36. Shannon, C.E. Communication in the Presence of Noise. *Proc. IEEE* **1998**, *86*, 447–457. [CrossRef]
37. Lai, E. 2-Converting Analog to Digital Signals and Vice Versa. In *Practical Digital Signal Processing*; Lai, E., Ed.; Newnes: Oxford, UK, 2003; pp. 14–49, ISBN 978-0-7506-5798-3.
38. WaveShare GitHub Repository. Available online: https://github.com/waveshare/High-Precision-AD-DA-Board/tree/master/Raspberry%20PI (accessed on 12 January 2023).
39. Leens, F. An Introduction to I2C and SPI Protocols. *IEEE Instrum. Meas. Mag.* **2009**, *12*, 8–13. [CrossRef]
40. Wolf, M. Chapter 2-Transistors and Integrated Circuits. In *the Physics of Computing*; Wolf, M., Ed.; Morgan Kaufmann: Boston, MA, USA, 2017; pp. 13–62, ISBN 978-0-12-809381-8.
41. Fleckenstein, C.J.; Gill, D.H.; Hemmendinger, D.; Mccreary, C.L.; Mcgregor, J.D.; Pargas, R.P.; Riehl, A.M.; Wallentine, V. Multiprocessing. In *Advances in Computers*; Yovits, M.C., Ed.; Elsevier: Amsterdam, The Netherlands, 1992; Volume 35, pp. 255–324, ISBN 0065-2458.
42. More, J.; Stieber, A.J.; Liu, C. Chapter 4.7-Community Support (Documentation, Bug Prioritization, Project Management). In *Breaking Into Information Security*; More, J., Stieber, A.J., Liu, C., Eds.; Syngress: Boston, MA, USA, 2016; pp. 208–209, ISBN 978-0-12-800783-9.
43. Williams, R. A Multiprocessing System for the Direct Execution of LISP. In Proceedings of the Fourth Workshop on Computer Architecture for Non-Numeric Processing, New York, NY, USA, 1–4 August 1978; Association for Computing Machinery: New York, NY, USA; pp. 35–41.
44. Sterling, T.; Anderson, M.; Brodowicz, M. Chapter 2-HPC Architecture 1: Systems and Technologies. In *High Performance Computing*; Sterling, T., Anderson, M., Brodowicz, M., Eds.; Morgan Kaufmann: Boston, MA, USA, 2018; pp. 43–82, ISBN 978-0-12-420158-3.
45. Yadav, M.; Singh, B.K.; Kumar, S. Framework for Managing Servers or Cluster of Servers Hardware Controlled by Raspberry Pi or Servers. In Proceedings of the 2020 IEEE International Conference for Innovation in Technology, INOCON 2020, Bangluru, India, 6–8 November 2020; Institute of Electrical and Electronics Engineers Inc.: Piscataway, NJ, USA.
46. Mas, J.; Panadero, T.; Botella, G.; del Barrio, A.A.; García, C. CNN Inference Acceleration Using Low-Power Devices for Human Monitoring and Security Scenarios. *Comput. Electr. Eng.* **2020**, *88*, 106859. [CrossRef] [PubMed]
47. Python Multiprocessing Library. Available online: https://docs.python.org/3/library/multiprocessing.html (accessed on 5 February 2023).
48. Carini, M.R.; Rocha, M.M. CESSIPy: A Python Open-Source Module for Stochastic System Identification in Civil Engineering. *SoftwareX* **2022**, *18*, 101091. [CrossRef]
49. Ribeiro, R.R. Micro EMM-ARM Repository in GitHub. Available online: https://github.com/renr3/microEMMARM/tree/main/V0.1.b-Synercrete23 (accessed on 24 February 2023).
50. Secil Redur-Multi. Available online: https://www.secil.pt/fr/produits/mortiers/revetements%20/redur-multi (accessed on 12 February 2023).
51. Regtien, P.; Dertien, E. 3-Uncertainty Aspects. In *Sensors for Mechatronics*, 2nd ed.; Regtien, P., Dertien, E., Eds.; Elsevier: Amsterdam, The Netherlands, 2018; pp. 39–60, ISBN 978-0-12-813810-6.